Organic Process Research & Development **2006**, *10,* 409–416

Modeling the Scale-Up of Contact Drying Processes

L. Hoekstra,[†] P. Vonk,[‡] and L. A. Hulshof*[,†,‡]

Eindhoven University of Technology, Laboratory of Macromolecular and Organic Chemistry, P.O. Box 513, 5600 MB Eindhoven, The Netherlands, and DSM Research, ACES Group, P.O. Box 18, 6160 MD Geleen, The Netherlands

Abstract:

The conventional way of scaling up a contact drying process includes a pilot-scale step. Scaling up from lab scale to production scale without the use of a pilot plant saves time and money. A method has been developed to perform a scale-up from a 200-g bench-scale Rotavap drying process to production scale (approximately 1000 kg). A mathematical model, an improvement on the so-called Schlünder model, has been developed to simulate bench-scale drying processes. This simulation is used to determine the unknown mixing parameters by regression analysis. Besides the heat transfer resistances predicted by Schlünder an additional resistance term was found which is product dependent and can also be determined by regression. Ultimately the model can be used to predict the drying curve on production scale. In five out of eight cases the developed method accurately predicted drying behaviour. In three remaining cases the model did not apply due to extreme stickiness or aggregation during drying.

Introduction

Fine chemicals are usually produced in multipurpose batch or semi-batch equipment, whereas bulk chemicals are produced in a dedicated continuously operated plant. Fine chemicals also experience short time-to-market and relatively short lifetime in the market as compared to bulk chemicals. Consequently, process research and development for the production of fine chemicals calls for a different approach that is even more challenging in view of the lack of appropriate design tools and generic methodologies for scale-up. Particularly, a fast and systematic approach is required for batch-drying processes that allow an early recognition of scale-up issues before process implementation on industrial scale.

Drying is one of the most energy-consuming steps in the production of solid-phase materials.[1] Consideration of this unit operation at an early stage of process development is an essential element in the design of a production process for a new pharmaceutical product.

During large-scale drying in contact dryers the heat is supplied through the wall of the dryer, and the main heat transfer mechanism is conduction. Usually this type of dryer operates under vacuum and may have devices to enhance mixing inside the dryer.

The conventional way of designing such a process [2] consists of three steps. First, preliminary experiments are performed at a laboratory scale to see how the product behaves. Then the product is tested in a pilot-scale dryer at typical batch sizes of 250−500 kg. The process is then scaled up to a larger scale (above 1000 kg). It is important to note that in general the dryer is part of a multipurpose plant. Such a plant may be used for a wide range of products, but the dryer cannot be redesigned for every new product. The dryer sizes are fixed, and the main design variables are jacket temperature, rotational speed, and operating pressure.

The goal of this work is to develop a method that can predict the performance of drying processes for any product, from bench scale to production scale without the use of a pilot-scale step. Such a method would have several major advantages. First, the pilot-scale phase is no longer needed, which means a large reduction in cost. Second, scale-up can be accomplished more quickly, resulting in a shorter time-to-market. Finally, the drying behaviour of the product at production scale can be determined in an early stage, when there is still only a small amount of the product available (only a few hundred grams will be enough to perform the required tests).

To predict the drying curve on production scale a two-step strategy is used. In the first step drying experiments are performed in a Rotavap (500-mL volume) at different rotation speeds. From these experiments a drying curve and a temperature curve are generated. Second, a simulation model has been written in VisualBasic/Excel to simulate these curves and extrapolate to a large-scale performance. This program uses the experimental data as input parameters and can be used to calculate unknown heat transfer parameters by regression analysis. Once these parameters have been determined, it is possible to estimate the drying curve on production scale.

The basis of this simulation program is the so-called Schlünder model that is developed by Schlünder from the University of Karlsruhe, Germany.[3−6]

The Schlünder Model

The Schlünder model has been used to describe the drying process of free-flowing powders on bench scale, based on penetration theory.[3−6] To describe the mixing process, a continuing cycle of static periods followed by perfect mixing is assumed. The drying process is thus modelled by means of a simulation program.

* Author for correspondence. E-mail: l.a.hulshof@tue.nl.
† Eindhoven University of Technology.
‡ DSM Research, ACES group.

(1) van 't Land, C. M. *Industrial drying equipment: selection and application*; Marcel Dekker: New York, Basel, Hong Kong, 1991.

(2) Moyers, C. G. *Evaluating Dryers for New Services*; CEP magazine, December 2003.

10.1021/op058014i CCC: $33.50
Published on Web 04/25/2006

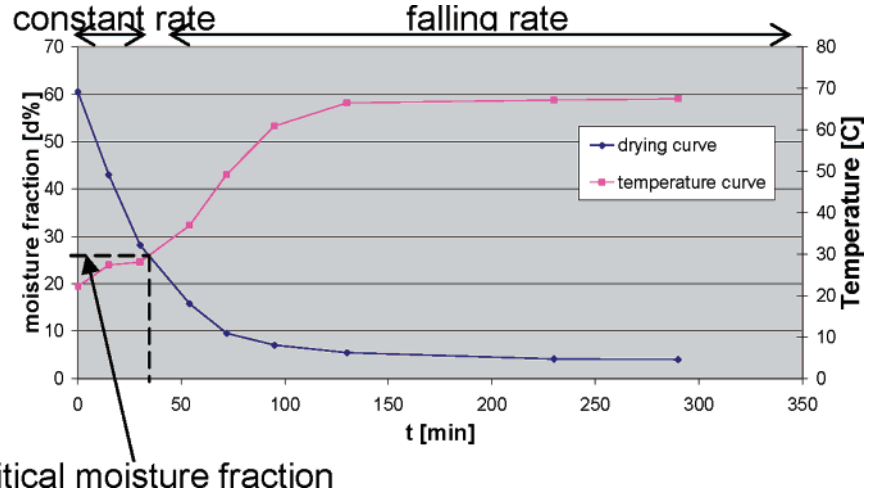

Figure 1. **Bench-scale drying of product E at $n = 4.8$ rpm, constant rate period from $t = 0$ to 40 min, falling-rate period from $t = 40$ min to ∞.**

The drying process consists of two phases (see Figure 1). The first phase is the constant-rate period. During this phase the product is still fairly wet, and the evaporation rate is constant, limited by the external rate of heat transfer. The drying curve appears as a straight line. The product temperature during this phase is equal to the boiling point of the liquid fraction at the operating pressure. The second phase is the so-called falling-rate period. During this period the drying rate decreases and asymptotically approaches zero if the equilibrium moisture fraction is reached. The liquid evaporated in this period is bound more tightly to the product on the surface and in the pores inside the particles, resulting in a lower vapour pressure and consequently a higher boiling point. The bed temperature will rise during this phase.

The moisture fraction that determines the transition from the first to the second phase is called the "the critical moisture content". This fraction is a characteristic of the product and can be easily determined from an experimental drying curve.

The model describes the drying process as a penetration process. It is assumed that there is a drying front that moves from the equipment wall into the bulk solid, parallel to the wall. Particles between the drying front and the wall are assumed to be completely dry, and particles beyond the drying front are assumed to be completely wet. This is shown schematically in Figure 2.

The heated surface is shown at the bottom. Below the drying front there is a layer of dry solids with zero moisture content. Above the drying front a layer of wet solids is shown in black. This layer of wet solids is assumed to be at boiling temperature at the prevailing pressure. The vapour phase consists of the pure liquid component. The amount of heat

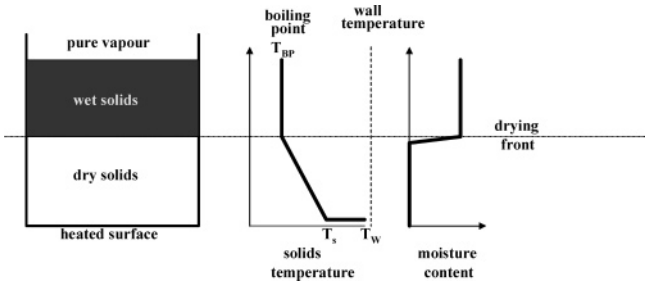

Figure 2. **Drying of nonhygroscopic material in a contact dryer: schematic representation, temperature profile, and moisture content profile.**

that is supplied to the particle bed can be calculated from the general formula:

$$Q = UA(T_{HM} - T_{bed}) \tag{1}$$

where Q is the heat supplied in joules per second [W], U is the overall heat transfer coefficient [W/m^2 K], A is the heating surface area [m^2], T_{HM} [K] is the temperature of the heating medium, and T_{bed} [K] is the bulk temperature of the bulk solids bed.

The overall heat transfer coefficient is determined by the individual heat transfer coefficients according to eq 2 and consists of five parts.

$$\frac{1}{U} = \frac{1}{h_{wall}} + \frac{1}{h_{ws}} + \frac{1}{h_{sb}} + \frac{1}{h_e} + \frac{1}{h_{add}} \tag{2}$$

The first term h_{wall} is the heat transfer coefficient of the wall of the dryer and can be calculated from eq 3 if the conductivity k [W/m K] of the wall material and the wall thickness d [m] is known. For a standard 500-mL glass Rotavap flask the value for h_{wall} has been determined to be 385 W/m^2 K as derived from the known thermal conductivity of glass and the thickness of the glass used in the Rotavap.

$$h_{wall} = \frac{k}{d} \tag{3}$$

The second term h_{ws} is the heat transfer coefficient from the wall to the first layer of particles. This contact heat transfer

(3) Mollekopf, N. *W*ärmeübertragung an mechanisch durchmischtes Schüttgut mit Wärmesenken in Kontaktapparaten. Ph.D. Thesis, Universität Frideriana Karlsruhe (Technische Hochschule), 1983.
(4) Oakley, D. E. *SPS Drying manual, Volume VII: Contact and layer drying, part 3: State of the science*; Separation AEA Technology plc, Harwell Laboratory, 1997.
(5) Schlünder, E. U.; Mollekopf, N. Vacuum Contact Drying of Free Flowing Mechanically Agitated Particulate Material. *Chem. Eng. Process.* **1984**, *18*, 93−111.
(6) Schlünder, E. U.; Tsotsas, E. *Wärmeübertragung in Festbetten, durchmischten Schüttgütern und Wirbelschichten*; George Thieme Verlag: Stuttgart, New York, 1988.

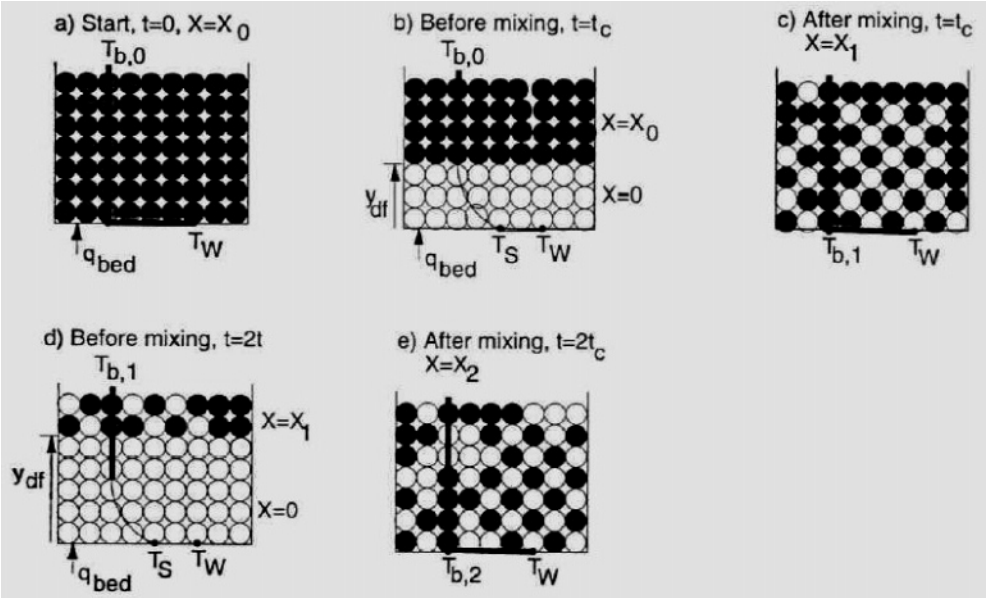

Figure 3. **Schlünders mixing model where t_c is the hypothetical contact time, a measure for the degree of mixing.[5,6,13]**

coefficient is independent of the mixing. It depends mainly on the characteristics of the product and to a weak extent on the characteristics of the inner surface of the apparatus. The contact heat transfer coefficient h_{ws} for a free-flowing powder can be estimated from existing correlations found in the literature.[4,6] It is independent of the agitation, see eq 4. Schlünder proposes the following correlation:[6]

$$h_{ws} = \psi_a h_{wp} + (1 - \psi_a)\frac{2K_g/d_p}{\sqrt{2} + 2(l + \Delta)/d_p} + h_{rad} + h_{dir} \quad (4)$$

where:

ψ_a = plate surface coverage (~0.8)[18]
K_g = gas thermal conductivity [W/m K] of solvent vapour
d_p = mean particle diameter [m]
Δ = surface roughness [m]
l = modified mean free path of the gas molecules [m]
h_{wp} = heat transfer from the wall to a single particle [W/m^2 K]
h_{rad} = heat transfer by radiation [W/m^2 K]
h_{dir} = heat transfer due to direct solid−solid conduction [W/m^2 K]

l, h_{wp}, h_{rad}, and h_{dir} can be calculated directly from the physical properties[18] of the solid, the vapour, and the wall.

The third term h_{sb} is the heat transfer coefficient from the first layer of particles to the bulk. h_{sb} is the component of U that depends on the mixing characteristics. h_{sb} is calculated according to eq 5. Equation 5 is the analytical solution of the Fourier equation as proposed by Neumann.[7]

$$h_{sb} = \frac{2}{\sqrt{\pi}}\sqrt{\frac{(KC_p\rho)_{bed}}{t_c}}\frac{1}{erf\zeta} \quad (5)$$

where K [W/m K], C_p [J/kg K], and ρ [kg/m^3] are the thermal conductivity, the specific heat, and the density of the bed, respectively. *erf* is the error function. t_c is the theoretical contact time, dependent on the mixing. The physical meaning of this contact time t_c is depicted in Figure 3 [5,6,13]. The thermal conductivity of the particles was estimated to be 0.75 W/m K.

The contact time t_c depends on the scale and operational conditions of the dryer. The effect of the size and operating conditions can be taken into account using the Froude number defined as:

$$Fr = \frac{(2\pi n)^2 D}{2g} \quad (6)$$

where D is the diameter of the equipment [m], g is the gravitational constant [m/s^2], and n is rotational speed in rps. Schlünder proposed the following relation between the contact time (t_c) and the Froude number (Fr):

$$t_c = \frac{N_{mix}}{n} \quad \text{where} \quad N_{mix} = C(Fr)^d \quad (7)$$

C and d are the so-called mix parameters and must be determined experimentally. ζ, in eq 5, is the dimensionless position of the drying front and is defined according to eq 8.

$$\zeta = \frac{y_{df}}{2\sqrt{(K/C_p\rho)_{bed}\,t}} \quad (8)$$

where y_{df} is the distance from the drying front to the heating surface.

In the fourth term of eq 2, h_e is the external heat transfer coefficient from the heating medium to the wall. Its value is large (estimated to be approximately 2000 W/m^2 K in all cases), and thus its contribution to U is relatively small. A more accurate estimation is not required.

The fifth term of eq 2, h_{add}, accounts for the additional heat transfer resistance that is product dependent but not related to the intensity of mixing. Its physical meaning is not fully understood, but it is assumed to reflect the

(7) Carslaw, H. S.; Jaeger, J. C. *Conduction of heat in solids*, 2nd ed.; Clarendon Press: New York, 1993.

Table 1. **Summary of products that were tested**

product	solvent	type of dryer
A: lanthanum carbonate, $La_2(CO_3)_3 \cdot 4H_2O$[15]	water	tumbler dryer
B: a heterocyclic aromatic carboxylic acid	water	filter dryer
C: a racemic heterocyclic aromatic amino acid derivative	water	filter dryer
D: a cyclic-1.3-dione	*n*-butyl acetate (98%) + water (2%)	Loediger dryer I
E: an acrylate polymer	water (88%) + 2-propanol (12%)	Loediger dryer I
F: a lithium salt of an alkyl-1,3-*N*,*N*-disubstituted-2-oxo-4,5-imidazolidine-dicarboxylate	water (50%) + toluene (50%)	Loediger dryer II
G: an N-carboxymethyl protected (*S*)-amino acid	water	filter dryer
H: a vitamin C derivative	acetone (88%) + methanol (12%)	filter dryer

interaction between the moisture and the solid at higher-moisture fractions during the constant rate period. h_{add} must be determined experimentally.

The drying rate can now be calculated according to eq 9.

$$W_{ev} = \frac{AU(T_{HM} - T_b)}{\lambda} \exp(-\zeta^2) \qquad (9)$$

where:

W_{ev} = evaporation rate [kg/s]
A = heat transfer surface [m^2]
U = overall heat transfer coefficient [W/m^2 K]
T_{HM} = temperature of heating medium [K]
T_b = temperature of the bulk [K]
λ = heat of vaporisation [J/kg]
ζ = reduced position of the drying front [-]

During the constant-rate period the boiling point of the moisture is calculated from the Antoine equation. The saturation pressure is taken equal to that of the free liquid. During the falling-rate period this ideal saturation pressure is lowered, depending on the moisture fraction according to eq 10.[16]

$$P_{vap} = (P_{vap,0})a_w \qquad (10)$$

where P_{vap} is the corrected vapour pressure and $P_{vap,0}$ is the vapour pressure calculated according to the Antoine equation. a_w is a number between 0 and 1 and is determined by the sorption isotherm. To estimate a_w the so-called BET isotherm is used.[8]

$$\frac{\omega}{\omega_{crit}} = \frac{C_B a_w}{(1 - a_w)(1 - a_w + C_B a_w)} \qquad (11)$$

ω is the moisture fraction, ω_{crit} is the critical moisture fraction, and C_B is the BET parameter.[17]

Determination of Model Parameters. Drying experiments were performed with eight products in an ordinary laboratory Rotavap setup. See Experimental Section for more details. Data were available for the commercial-scale drying behaviour for each of these products. The products and operating conditions are summarised in Tables 1 and 2. These experiments were performed to determine the unknown parameters of the model.

Table 2. **Operating conditions and solid properties (solubilities are given for the bath temperature)**

	T_{bath} [°C]	P [mbar]	solubility [wt %]	particle size [μm]
A	70	40	<0.1	44.5
B	70	40	<0.1	85.6
C	42	25	<0.1	65.7
D	44	25	7	16.8
E	75	35	<0.1	836
F	52	50	<0.1	9.9
G	43	30	4.2	21.9
H	33	30	6.9	50.2

The Schlünder model contains four unknown parameters: the additional heat transfer coefficient (h_{add}), the characteristic contact time (t_c), and mix parameters C and d. The characteristic contact time and the mix parameters can be related to each other by means of eq 7, reducing the number of unknown parameters to three. These three parameters can be estimated on the basis of experimental drying data.

Each individual experiment can be characterised by only two parameters: the additional heat transfer coefficient (h_{add}) and the characteristic contact time (t_c). These two parameters can be estimated for each individual experiment by minimising the quadratic difference between the experimental and simulated data. The so-called Levenberg−Marquardt method[9] was used for nonlinear regression.

The unknown mix parameters C and d from eq 7 are estimated using the estimated contact time values from the drying experiments at different rotation rates. Equation 7 can be rearranged into a linear relationship by applying natural logarithms.

$$\log N_{mix} = \log(t_c n) = \log C + d \log Fr \qquad (12)$$

Each of the products was dried at bench scale at three different rotation speeds, and for each experiment the characteristic contact time was estimated.

C and d can now be determined by plotting log N_{mix} against log Fr.

Results and Discussion

Table 3 summarises the results of the optimisations based on the bench-scale experiments.

(8) Allen, T. *Particle Size Measurement*, 4th ed.; Chapman & Hall: New York, 1993.

(9) Press, W. H.; Vetterling, W. T.; Teukolsky, S. A.; Flannery, B. P. *Numerical recipes in C, the Art of Scientific Computing*, 2nd ed.; Cambridge University Press: New York, 1992.

Table 3. **Calculated mix parameters and average h_{add}**

product	C	d	h_{add} [W/m^2 K]
A	45.7	−0.0824	95
B	0.0571	−1.02	61
C	7.9×10^4	1.05	314
D	2.04×10^{10}	3.07	25
E	478	0.37	131
F	1.89×10^4	0.27	572
G	43.24	−0.129	364
H	127.2	0.4455	274

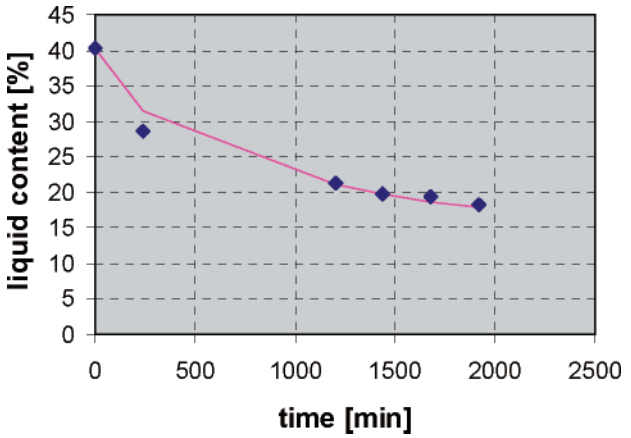

Figure 4. **Scale-up of drying of product A,[15] comparison of predicted drying curve with actual production scale data (tumbler dryer): solid line is predicted, dots are actual.**

According to Schlünder, C and d are constants for a given apparatus for free-flowing particles. From Table 3 it can be concluded that this does not apply in our cases. The mix parameters C and d are not the same for all the products despite the fact that they were measured in the same bench-scale equipment. The reason is that the behaviour of our products is not ideally free flowing. The particles of each of the products have a tendency to stick together to a degree that depends on the characteristics of the material and the moisture fraction. This means that the mixing of the product in the apparatus depends more on the nature of the specific product than on the equipment itself.

On the basis of the results in Table 3, two general rules were derived for the scale-up of drying processes. The first rule is that eq 13 can be applied both on small and on large scale (see also eqs 7 and 12).

$$N_{mix} = C(Fr)^d \tag{13}$$

The mix parameters C and d can be determined from the lab experiments by plotting log N_{mix} against $\log((2\pi n)^2 D/2g)$. N_{mix} is determined through optimisation of the contact time.

The second rule is that the empirical parameter h_{add} is only product dependent and is the same for small and large scales.

The results of the scale-up drying time predictions for several products are given in Figures 4 to 11. The solid line represents the predicted drying curve based on laboratory drying data. The dots represent the actual production scale data. The dashed line represents the predicted composition

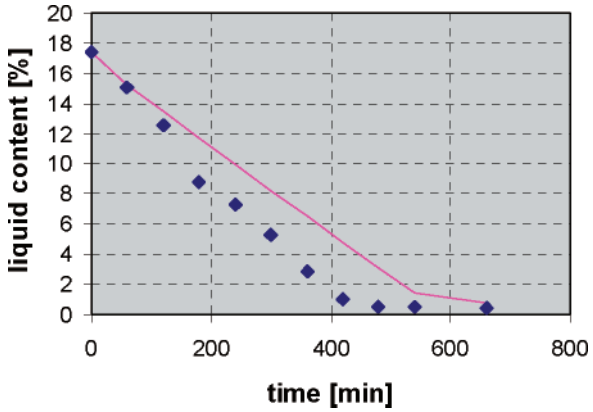

Figure 5. **Scale-up of drying of product B, comparison of predicted drying curve with actual production scale data: solid line is predicted, dots are actual.**

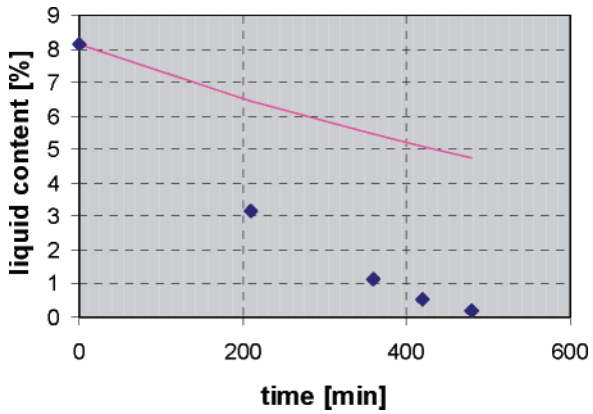

Figure 6. **Scale-up of drying of product C, comparison of predicted drying curve with actual production scale data: solid line is predicted, dots are actual.**

of the moisture fraction in case of more than one liquid component.

As can be seen from the graphs, for products A, E, G, and H the curve that was derived from the laboratory experiments is in good agreement with the actual production process data. Also for product B the agreement between predicted and actual is quite satisfactory, although the actual drying time is a bit shorter than the predicted drying time.

Since product A is dried in a tumbler dryer, products B, G, and H in filter dryers, and product E in a Loediger dryer, it seems that satisfactory predictions of the drying time can be made in three very different types of contact dryer.

Exceptions for Products C, D, and F. Still the production-scale drying curves of products C, D, and F were not well predicted using the proposed method. During the drying experiments of product C, intense stickiness of the wet product was observed on bench scale. The product formed one large porous paste-like lump until it was almost dry. The rotating motion of the Rotavap was not able to break this lump until the final stages of drying. When the product was almost dry, the lump fell apart. The same behaviour was observed for all three rotation rates. This indicates that the mixing process hardly depends on the rotation speed.

Mixing of product C at production scale is much better than expected from the lab results, due to the mechanical action of a rotating scraper. This facilitates the drying

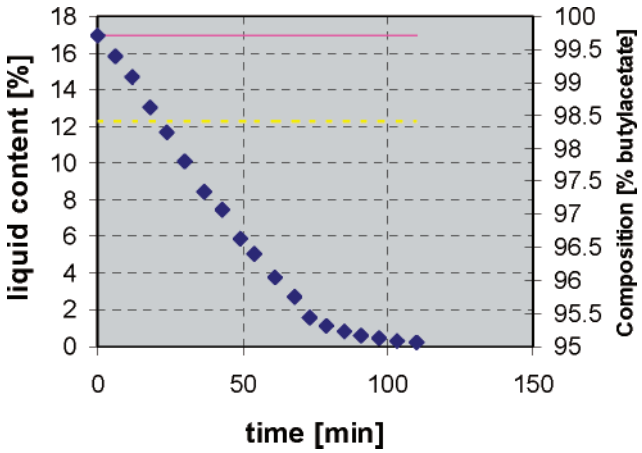

Figure 7. **Scale-up of drying of product D, comparison of predicted drying curve with actual production scale data: solid line is predicted, dots are actual, and yellow line represents the calculated composition of the liquid in the solid residue.**

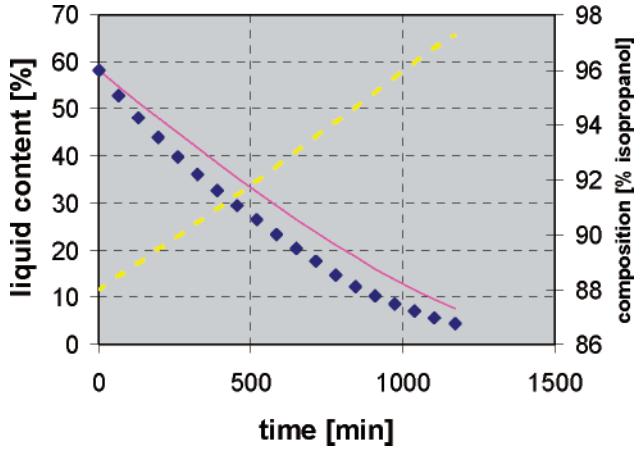

Figure 8. **Scale-up of drying of product E, comparison of predicted drying curve with actual production scale data: solid line is predicted, dots are actual, and yellow line represents the calculated composition of the liquid in the solid residue.**

process. The difference in behaviour between small and large scale arises because the product is not free-flowing.

For product D another phenomenon occurs. At first sight the product seems to behave like a free-flowing powder. However, unexpectedly, bench-scale experiments showed that the drying time increases when the rotation speed is increased. For this product, the simulation incorrectly predicts that drying is not possible, although drying has been accomplished at large scale (compare predicted and actual curves in Figure 7).

The reason for this strange effect at bench scale is probably the formation of small aggregates or clusters due to the rotation of the flask. Such aggregation hinders the drying process, probably because of increased heat or mass transfer resistance. Presumably, aggregation increases as the rotation rate is increased. Consequently, the drying process will be slower at a higher rotation rate. Clearly, the model does not apply to this case.

A similar observation was made with product F (see Figure 9). Here, the formation of aggregates can actually be seen during the drying process. As can be derived from

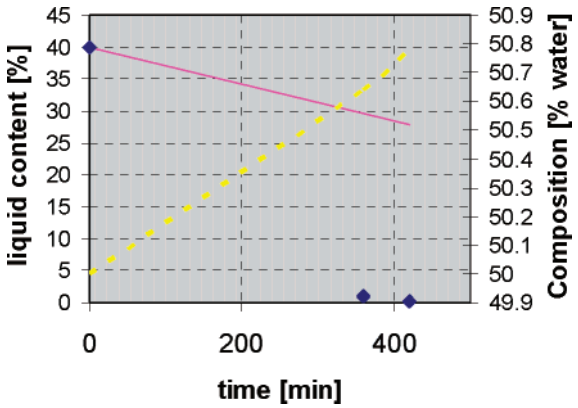

Figure 9. **Scale-up of drying of product F, comparison of predicted drying curve with actual production scale data: solid line is predicted, dots are actual, and yellow line represents the calculated composition of the liquid in the solid residue.**

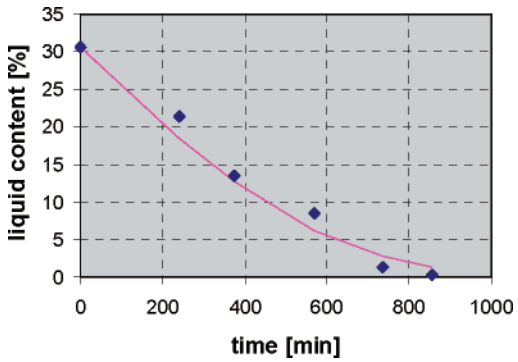

Figure 10. **Scale-up of drying of product G, comparison of predicted drying curve with actual production scale data: solid line is predicted, dots are actual.**

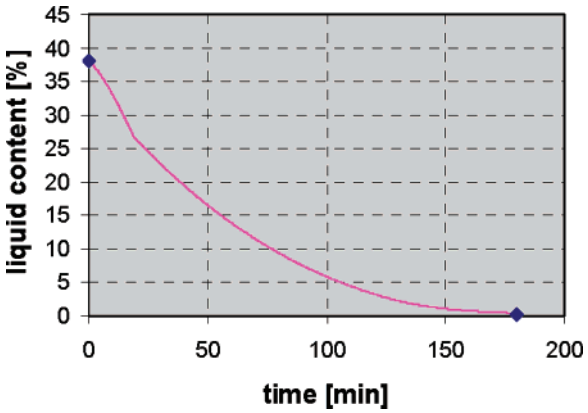

Figure 11. **Scale-up of drying of product H, comparison of predicted drying curve with actual starting and final moisture fraction at production scale: solid line is predicted, dots are actual.**

eqs 6 and 7 the following relation holds:

$$t_c \approx n^{2d-1} \tag{14}$$

t_c is the contact time and can be taken as a measure of the intensity of mixing. If the contact time is shorter, the mixing is considered to be better. The mixing becomes ideal if t_c approaches zero. Table 4 lists the calculated values of t_c for all bench-scale experiments as well as the t_c for the production scale curves. Under "normal" circumstances, t_c

Table 4. **Values of contact time t_c in minutes for bench scale and production scale (results are obtained through optimisation)**

product A:			product B:			product C:			product D:		
n [rpm]	scale	t_c [min]	n [rpm]	scale	t_c [min]	n [rpm]	scale	t_c [min]	n [rpm]	scale	t_c [min]
1.7	lab	49	2.9	lab	46	3.3	lab	35	2.77	lab	0.52
4.7	lab	23	4.4	lab	14	4.6	lab	44	4.96	lab	2.9
11.7	lab	4.32	8.1	lab	2.1	7.3	lab	43	9.01	lab	220
17	lab	4.25	6	prod	0.2	6	prod	7	46	prod	0.59
4	prod	0.11									

product E:			product F:			product G:			product H:		
n [rpm]	scale	t_c [min]	n [rpm]	scale	t_c [min]	n [rpm]	scale	t_c [min]	n [rpm]	scale	t_c [min]
3.21	lab	8.4	3.57	lab	727	4.46	lab	22.7	3.82	lab	1.47
4.77	lab	10.4	8.03	lab	516	6.55	lab	15.2	6.01	lab	1.21
8.29	lab	6.8	10.08	lab	449	9.29	lab	9.0	8.94	lab	1.35
23	prod	2.3	30	prod	0.13	6	prod	10.7	30	prod	4.6

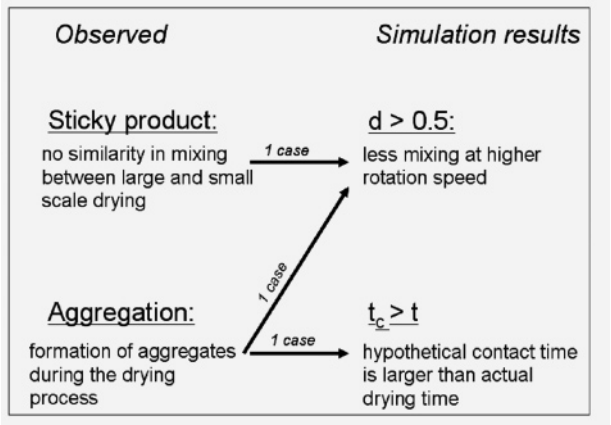

Figure 12. **Causes of failure cases of the proposed scale-up method.**

would be expected to decrease with increasing rotation speed resulting in a value of d smaller than 0.5. Note, however, that for both products C and D the values of d are higher than 0.5 (see Table 3). This means that mixing appears worse at higher rotation rates, and consequently the drying is slower. It can be concluded that in both cases the mixing model is not suitable for prediction purposes. If the value of d is larger than 0.5, the proposed method cannot be used.

For product F, the value of d is slightly lower than 0.5 (e.g., 0.27), but from Table 4 it can be concluded that the value of t_c exceeds the drying time itself. The simulation program sees aggregation formation as an example of bad mixing and concludes that this is even worse than no mixing at all. Apparently, the mixing model is not suitable for this case either. If the optimised value of t_c is larger than the actual drying time, again this prediction method cannot be used.

The lack of suitability of the model for these three cases could be anticipated from the results of the regression optimisation and the experimental behaviour of the products in the Rotavap. This is schematically pictured in Figure 12.

Conclusion

On the basis of the Schlünder model a method was developed to directly predict the behaviour of contact drying processes at production scale (500−2500 kg) based on bench-scale data (approximately 200 g). Working with these small bench-scale quantities is essential during the early stages of fine chemical process research and development. With this method the production-scale drying curve can be predicted based on bench-scale experiments within 15% accuracy for ordinary cases. Ordinary free-flowing powders show similar behaviour on large and small scale and are not influenced by physical phenomena such as aggregation. In agreement with previous work[10−14] it was found that the drying curve of a contact drying process can be described well with the Schlünder model both at bench- and production scale, even when the product is not an ideally free-flowing powder as long as aggregation was not a serious problem. Nevertheless, introduction of an additional heat transfer coefficient term beyond those considered by the Schlünder model was needed for a good prediction. This additional heat transfer coefficient was called h_{add}.

It was found that the characteristic mixing parameters for prediction are only product dependent. This result is not in agreement with Schlünders conclusion that these parameters are equipment dependent. Our work shows that mixing

(10) Chen, X. D. On the Characteristic Drying Rate Approach to Correlation Experimental Results of the Drying of Moist Porous Materials. *Can. J. Chem. Eng.* **2002**, *80*, 984−990.

(11) Dittler, A.; Bamberger, T.; Gehrmann, D.; Schlünder, E. U. Measurement and Simulation of the Vacuum Contact Drying of Pastes in a LIST-Type Dryer. *Chem. Eng. Process.* **1997**, *36*, 301−308.

(12) Gevaudan, A.; Andrieu, J. Contact Drying Modelling of Agitated Porous Alumina Beads. *Chem. Eng. Process.* **1991**, *30*, 31−37.

(13) Thurner, F.; Schlünder, E. U. Progress towards Understanding the Drying of Porous Materials Wetted with Binary Mixtures, *Chem. Eng. Process.* **1986**, *20*, 9−25.

(14) Tsotsas, E. Über den Einfluss der Dispersität und der Hygroskopizität auf ein Trocknungsverluf bei der Vakuum-Kontakttrocknung rieselfähiger Trocknungsgüter. Ph.D. Thesis, Universität Fridericiana Karlsruhe (Technische Hochschule), 1985.

(15) Lanthanum carbonate ($La_2(CO_3)_3$, CAS number 54451-24-0, wet: $La_2(CO_3)_3 \cdot 8\ H_2O$, after drying: $La_2(CO_3)_3 \cdot 4\ H_2O$, molar mass: 0.6 kg/mol, average particle size: 44.5 μm, bulk density: 717 kg/m^3, true density: 2650 kg/m^3, moisture fraction: water, initial moisture fraction: 0.40 kg/kg dry solid.

(16) The constant rate period has been approached by $P_{vap}(t) = \sum x_i(t) * P_{vap,\ i,0}$ where $P_{vap}(t)$ is the vapour pressure of the mixture at point t in time, while $P_{vap,0}$ is the vapour pressure of the pure component (depending on the temperature) and x_i is the calculated mol fraction of component i in the remaining liquid at point t in time.

(17) Brunauer, S.; Emmett, P. H.; Teller, E. Adsorption of Gases in Multimolecular Layers. *J. Am. Chem. Soc.* **1938**, *60*, 309−319.

(18) Schlünder, E. U. *VDI-WÄRMEATLAS*; VDI−Verlag Gmbh: Dûsseldorf, Germany, 1984.

depends more on the characteristics of the product than on the apparatus for non-free-flowing powders. The additional heat transfer coefficient was found to be product dependent.

The proposed scale-up method gave good results in five out of eight cases. Good results were obtained for three different types of contact dryer: a tumbler dryer, a filter dryer, and a Loediger dryer. We conclude that this estimation method can be used for each type of contact dryer.

The scale-up method failed to predict drying behaviour in three cases. In one, the product was so sticky that it formed one big lump in the Rotavap. Even in the production-scale filter dryer, mixing was difficult for this product, although more effective than in the Rotavap. In the two other unsuccessful cases, aggregation occurred during the drying process in the Rotavap. Formation of aggregates increases with increasing rotation speed and hinders the drying process. This effect could not be described by the Schlünder model.

Experimental Section

The bench-scale drying experiments were performed in an ordinary Rotavap dryer. The wet product was dried in a baffled 500-mL glass flask. The flask had four ridges in the wall to improve the mixing during rotation. In all cases, the flask was filled to 50% of its volume with wet or rewetted product and submerged in the water bath. By approximation the heat transfer area was taken as half the surface area of the flask.

The rotation speed, the bath temperature, and the pressure inside the flask could be controlled. The powder temperature was measured continuously during the experiment by means of a thermocouple. For each product at least three bench-scale experiments were performed at three different rotation rates.

At certain time intervals during the drying experiments samples were taken, and the powder temperature was recorded. The moisture content was determined gravimetrically by weighing before and after drying overnight in an oven at a temperature 5 °C higher than the boiling point of the liquid that had to be removed. It was assumed that the product was completely dry after one night of drying. In the case of product D the moisture fraction of the product was not determined gravimetrically but by gas chromatography. No degradation of products has been observed.

Eight products were examined in this way. Data were available for the commercial-scale drying behaviour for each of these products. The products are summarised in Table 1.

Symbols Defined

Symbol = description [unit]

A = heat transfer area [m^2]

a_w = sorption activity [-]

C = mix parameter [-]

C_B = BET adsorption coefficient [-]

$C_{p,bed}$ = heat capacity of the bed [J/kg K]

D = diameter of the dryer [m]

d = mix parameter [-]

d = wall thickness [m]

d_p = average particle diameter [m]

Fr = Froude number [-]

g = gravitational constant [m/s^2]

h_{add} = additional heat transfer coefficient [W/m^2 K]

h_{sb} = heat transfer coefficient 1st particle layer to bulk [W/m^2 K]

h_{dir} = heat transfer coefficient from direct solid−solid contact [W/m^2 K]

h_e = external heat transfer coefficient [W/m^2 K]

h_{rad} = heat transfer coefficient due to radiation [W/m^2 K]

h_{wall} = wall heat transfer coefficient [W/m^2 K]

h_{wp} = heat transfer coefficient wall to single particle [W/m^2 K]

h_{ws} = heat transfer coefficient wall to 1st particle layer [W/m^2 K]

K_{bed} = thermal conductivity of the bed [W/mK]

K_g = thermal conductivity of the gas [W/m K]

k = thermal conductivity of the wall [W/m K]

l = modified mean free path length of a gas molecule [m]

N_{mix} = mixing number [-]

n = rotation speed [s^{-1}/min^{-1}]

P_{vap} = vapour pressure [Pa]

$P_{vap,0}$ = vapour pressure of the pure component (Antoine eq) [Pa]

Q = heat flow [W]

T_{bed} = bulk temperature of the bed [K]

t_c = hypothetical contact time [s]

T_{HM} = temperature of the heating medium [K]

U = overall heat transfer coefficient [W/m^2 K]

W_{ev} = evaporation rate [kg/s]

X = moisture fraction [-]

$x_{i,moist}$ = mol fraction of component i in the moisture fraction [-]

y_{df} = distance from the drying front to the wall [m]

Δ = surface roughness [m]

ζ = dimensionless position of the drying front [-]

λ = heat of vaporization [J/kg]

$\rho_{,bed}$ = density of the bed [kg/m^3]

ψ_a = plate surface coverage factor [-]

ω = moisture fraction (kg moisture per kg dry solid × 100%) [d%]

ω_{crit} = critical moisture fraction [d%]

Acknowledgment

We thank Prof. Dr. Ir. P. J. A. M. Kerkhof of the Eindhoven University of Technology and Ing. J. J. H. M. Lemmen of DSM Pharma Chemicals at Venlo for fruitful discussions and DSM Pharma Chemicals for financial support.

Received for review September 28, 2005.
OP058014I